

# MiniPIX Cosmic Ray Tracking and Radiation Dosimetry During SORA Stratospheric Balloon Flights

S. A. Garcia Morelos<sup>a,\*</sup>, A. Walker<sup>a,\*</sup>, R. B. Masek<sup>a</sup>, S. Oliver<sup>a</sup>, F. Brooks<sup>a</sup>,  
K. D. Portillo<sup>a</sup>, J. Patel<sup>a</sup>, D. Pattison<sup>b</sup>, A. L. Renshaw<sup>a</sup>

<sup>a</sup>*Department of Physics, University of Houston, Houston, TX 77204, USA*

<sup>b</sup>*Department of Biology and Microbiology, University of Houston, Houston, TX 77204, USA*

---

## Abstract

Results from two separate detector runs onboard the Stratospheric Organisms and Radiation Analyzer (SORA) high altitude balloon flights are presented. The SORA payload included a semiconductor pixel detector for cosmic ray studies and imaging in the stratosphere at altitudes between 30 and 40 kilometers. The MiniPIX was interfaced with a low-powered computer, a Raspberry Pi 3. The MiniPIX was set to TOT (time over threshold mode) and monitored cosmic radiation for a combined flight time of 19.5 hours on the two separate flights. The results from the SORA flights were evaluated for providing a basis for future low cost cosmic ray tracking platforms on high altitude balloons and satellites.

*Keywords:* MiniPIX, TimePIX, HASP, SORA, Cosmic Radiation, Stratospheric Balloon, Dosimetry

---

---

\*Corresponding authors

*Email addresses:* [sagarciamorelos@uh.edu](mailto:sagarciamorelos@uh.edu) (S. A. Garcia Morelos ),  
[andrewg.walker@outlook.com](mailto:andrewg.walker@outlook.com) (A. Walker )

## 1. Introduction

The atmospheric radiation environment is highly complex and is comprised mostly of a mix of primary and secondary particles originating from Galactic Cosmic Rays (GCRs). Primary GCRs interact with atoms and molecules in the Earth's upper atmosphere and produce cascades of secondary particles that increase in intensity until reaching a maximum between 16 km and 18 km, known as the Regener-Pfotzer Maximum[1]. After reaching peak ionization rates, the flux of secondary and primary particles decreases steadily while decreasing in altitude, until reaching a minimum near the Earth's surface. The increase in ionizing radiation with altitude has implications to passengers and crew aboard high flying aircraft and astronauts in low earth orbit (LEO), who will absorb a much higher biological dose than they would at the Earth's surface.

According to research from the Federal Aviation Administration (FAA) Civil Aerospace Medical Institute, passengers and crew onboard a flight from London to Los Angeles will be exposed to an average effective dose of 61.6  $\mu\text{Sv}$  [2]. Furthermore, measurements taken aboard the International Space Station (ISS) shows that ISS crew members can be exposed to dose rates on the order of 200  $\mu\text{Sv}$  per day. Exposure to high levels of ionizing radiation increases the risk of cancer and may be linked to other health risks such as increased rate of birth defects and miscarriages [3]. Additionally, data from the CRaTER cosmic ray telescope aboard NASA's Lunar Reconnaissance Orbiter has shown that dose rate from cosmic rays in the vicinity of the moon has reached the highest level observed since the beginning of the space age [4]. The health risks associated with exposure to radiation in the

atmosphere and in space combined with the increase in cosmic ray intensity during solar minimum periods point towards the necessity of the development of a relatively low cost device for monitoring the radiation environment in real-time.

The MiniPIX is a portable radiation camera developed by the TimePIX/MiniPIX Collaboration and commercialized by Advacam (CITE ME). It utilizes a 256x256 pixel silicon TimePIX Application Specific Integrated Circuit (ASIC) and a USB readout interface. The device can be operated under one of three modes: time-of-arrival (TOA), time-over-threshold (TOT), or single particle counting. The MiniPIX is capable of individual particle differentiation and when operating in TOT mode can be used to measure dosimetric endpoints such as absorbed dose and dose equivalent. Similar devices to the MiniPIX utilizing a TimePIX ASIC have been evaluated on high altitude balloon flights by Urbar et.al [5] and are currently deployed on the ISS for performing real-time space radiation monitoring [6]. However, the usage of the MiniPIX in combination with a low cost single board computer as a portable radiation monitoring device has yet to be fully explored. The SORA flights in 2017 and 2018 served as a test bed for such a system.

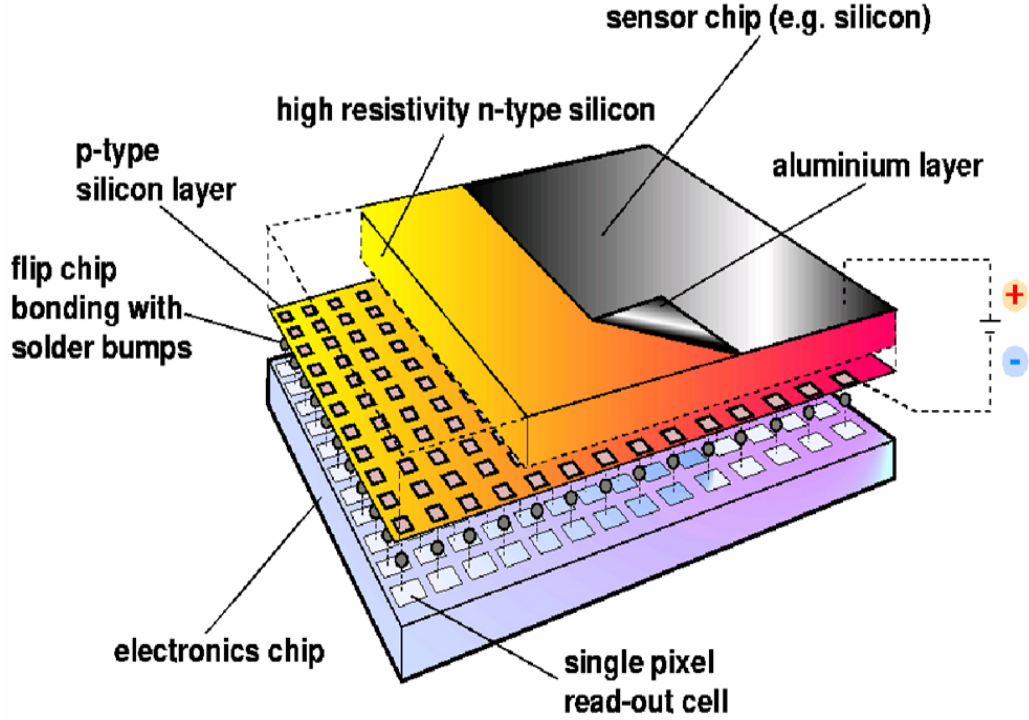


Figure 1: TimePIX detector structure concept design [7]

During the High Altitude Student Platform (HASP) 2017 and 2018 flights [8], the SORA payloads carried a MiniPIX interfaced with a Raspberry Pi 3 B+ (RPI) Single Board Computer (CITE ME) to test the feasibility of a system for real-time measurements of absorbed dose from cosmic radiation. Data, such as counts and absorbed dose from the MiniPIX, was downlinked and analyzed in real time through the HASP downlink interface. The HASP 2017 flight launched from Fort Sumner, New Mexico on September 4th, 2017 at 14:04 UTC and ascended to a float altitude of approximately 31.5 km at 16:22 UTC; which was maintained for approximately 10.5 h. The HASP 2017 payload drifted west for a total ground distance of 580 km and was

recovered just north of the Apache-Sitgreaves National Forest in Arizona. On September 4th, 2018 at 14:03 UTC the HASP 2018 mission launched from Fort Sumner, New Mexico. The 2018 payload reached a stable float altitude of 37.2 km at 16:30 UTC and the total float duration was approximately 9.0 h. The 2018 payload terminated its flight and landed approximately 96.6 km southwest of Mt Graham, Arizona after traveling a total distance of 550 km.

## 2. Methods

For the SORA flights, the MiniPIX was interfaced via USB with Raspberry Pi (RPI) single board computer. Data was collected on the MiniPIX and frame data was sent over serial to the RPI for analysis. During the 2017 flight, only the raw data was stored for post-flight analysis. For the 2018 flight, a custom piece of software was written to concurrently handle analyzing frame data, calculating absorbed dose and handling command and configuration requests from the HASP telemetry interface in addition to storing the raw data. The improvements in the 2018 flight allowed for a near real-time analysis of the radiation environment and the ability to configure the MiniPIX shutter rate and detector parameters via the HASP uplink interface. While being relatively cheap at a price point of 35\$ USD and consuming only 1.2 W of electrical power, the RPI proved to be robust and operated without glitch for the duration of both flights.

### *2.1. Configuration and Calibration*

The Timepix ASIC consists of 65,536 silicon p-n diodes, each containing its own individual processing circuit. The response of each pixel can never be identical, thus a calibration must be performed for each individual pixel.

The appropriate calibration of the MiniPIX detector was applied at The University of Houston following a calibration procedure outlined by Jakubek [18]. The source calibration was applied using the 60 keV  $^{241}\text{Am}$  decay line, Sn Fluorescence and  $^{55}\text{Fe}$  gamma rays.

## *2.2. System Design*

Additive manufacturing was used to create a custom made case for the MiniPIX device. The flight assembly is shown in Figure 2 with individual components as labeled. In the early vacuum tests, it was found that the MiniPIX would require a passive cooling method to keep its temperature within operating limits. At the same time, the ABS plastic enclosure acted as insulation, maintaining the MiniPIX temperature within the operating range. The MiniPIX was mated to the heatsink via a bracket (not shown in the figure 2) and with thermal adhesive.

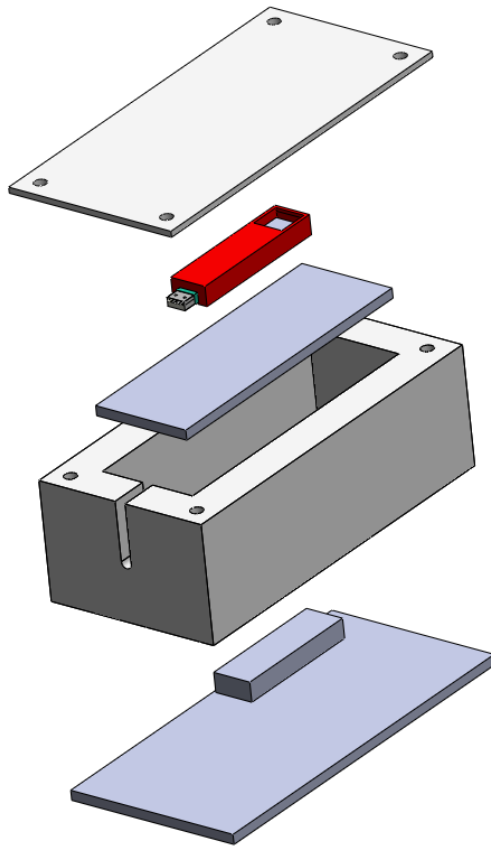


Figure 2: MiniPIX Case Assembly

The MiniPIX case allowed for a USB cable to be routed through the enclosure to interface directly to the Raspberry Pi. This allowed the MiniPIX device to be modular and placed in different configurations for the two flights. The Raspberry Pi was placed in a separate location within each payload near the power supply. Overall, each payload was modular and accessible.

### 3. Results

#### 3.1. Flight Data

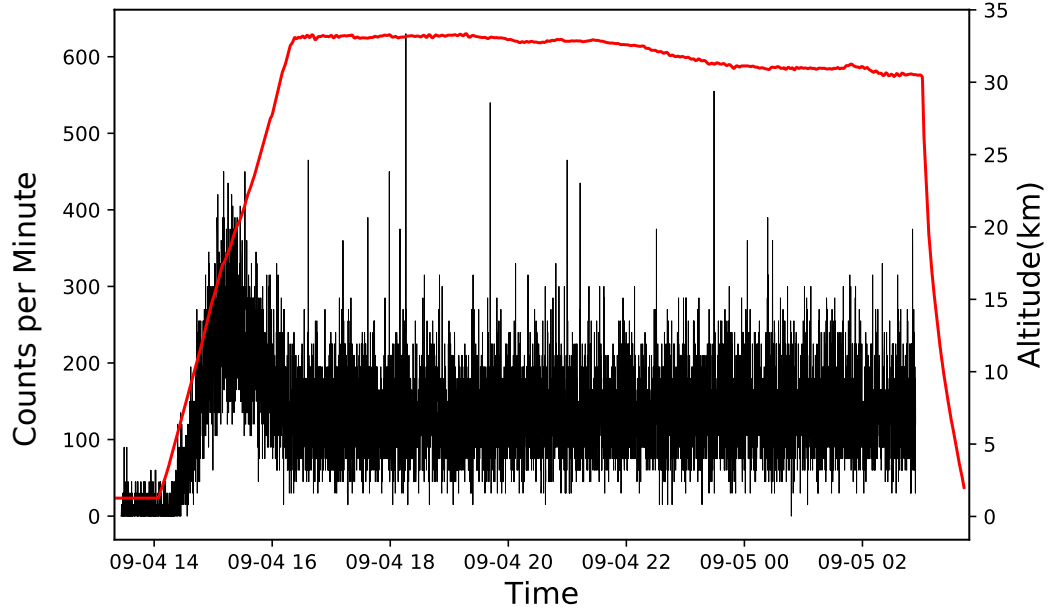


Figure 3: Count Rate and Altitude vs Time for 2017 flight. The red line represents the GPS altitude over time in km. The black lines represent the counts per minute over time

The MiniPIX was set to operate in Time over Threshold mode with a bias voltage of 4 keV. Frames were collected at static 4 second intervals during the 2017 flight and between 1 and 4 second intervals for the 2018 flight. The complete flight altitude profiles and count rates for the SORA 2017 and 2018 flights are shown in Figure 3 and Figure 4, respectively.



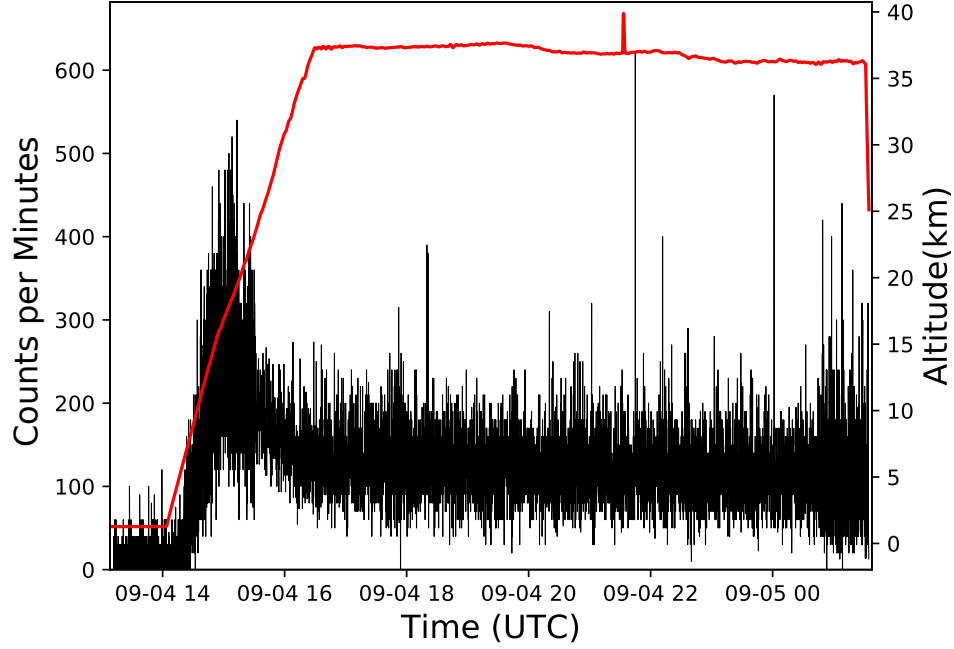


Figure 4: Count Rate and Altitude vs Time for 2018 flight. The red line represents the GPS altitude over time in km. The black lines represent the counts per minute over time

As shown in Figure 3 and Figure 4, both flights have very similar flight altitude profiles. Both flights reached a float altitude after approximately 2.5 h. It is important to mention that the 2017 float altitude was approximately 31.5 km. While that for the 2018 flight was about 37.2 km. The rate of decent was slow and steady for both flights. As such, data was collected continuously throughout the whole flights.

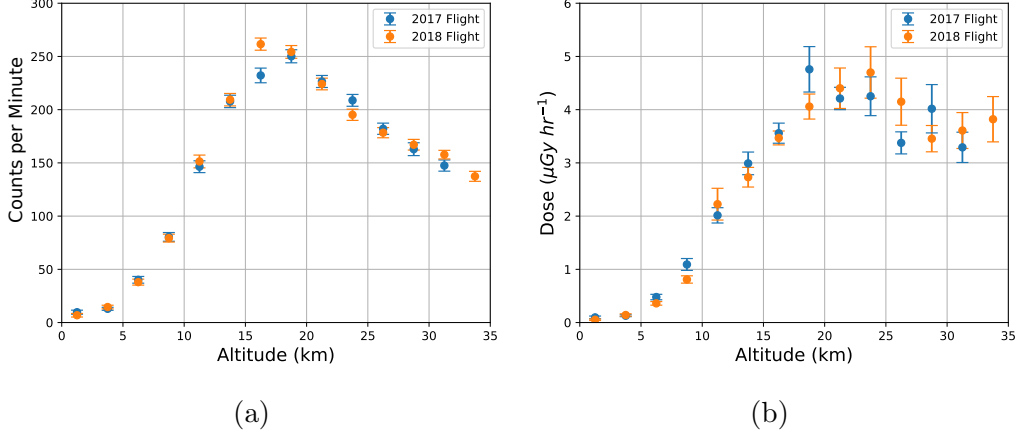


Figure 5: Figure 5a shows the detector counts per minute as a function of GPS altitude. Figure 5b shows the absorbed dose rate in silicon as a function of GPS altitude. Samples were averaged over 2.5 km bins and error bars for both plots represent the standard error of the mean plotted at the  $1\sigma$  level.

Shown in Figure 5b and Figure 5a are the dose rate in silicon and the detector count rate plotted as a function of GPS altitude. For the sake of clarity samples were averaged over 2.5 km bins and plotted with error bars representing the standard error of the mean at the  $1\sigma$  level. Dose rates for both flights appear to be in relatively good agreement up until approximately 16 km. After which, the 2017 flight appears to reach a peak dose rate of  $4.8 \mu\text{Gy h}^{-1}$  at approximately 18 km while the 2017 flight reaches a peak of  $4.8 \mu\text{Gy h}^{-1}$  at a higher altitude of 24 km. However, the large error bars indicate that it is somewhat unclear as to where the peak dose rate occurs for both flights. The count rates for both flights seem to be in much better agreement than the dose rates and show only a small discrepancy between 15 km and 17.5 km at which the 2018 flight experienced a count rate approximately 30 counts per

minute higher than that of the 2017 flight. With both flights reaching altitudes beyond 25.0 km, the Pfotzer-Regener maximum was clearly observed. In 2017, the Pfotzer-Regener maximum peaked at approximately 18 km. Similarly, the 2018 mission recorded Pfotzer-Regener maximum peaking around 20 km. After the observed peaks in count rate, the count rate tapered off inversely with rising altitude. These count rates then remained constant for the remainder of the flights.

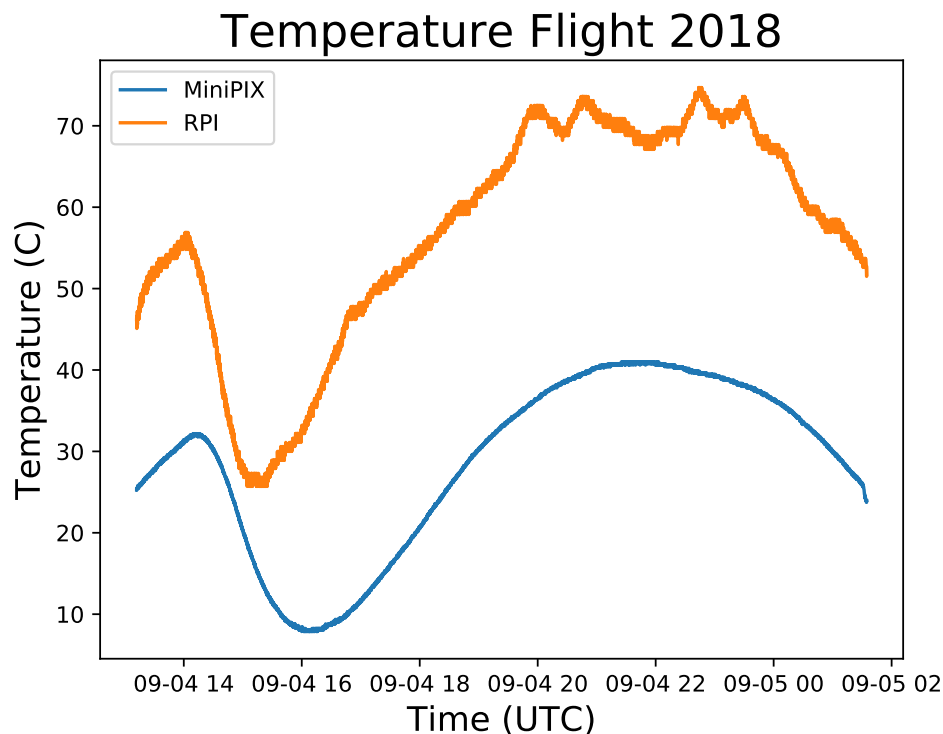


Figure 6: 2018 recorded temperatures of the MiniPIX and Raspberry Pi Flight computer.

The MiniPIX and RPI both operated well throughout both flights. The 2018 flight was better equipped to record system health and operation status.

A key status indicator of system health was the system temperature. These temperatures recorded are shown in Figure 6. The MiniPIX temperature stayed within expected ranges and never exceeded 40 °C. Likewise, the RPI stayed with operational temperatures.

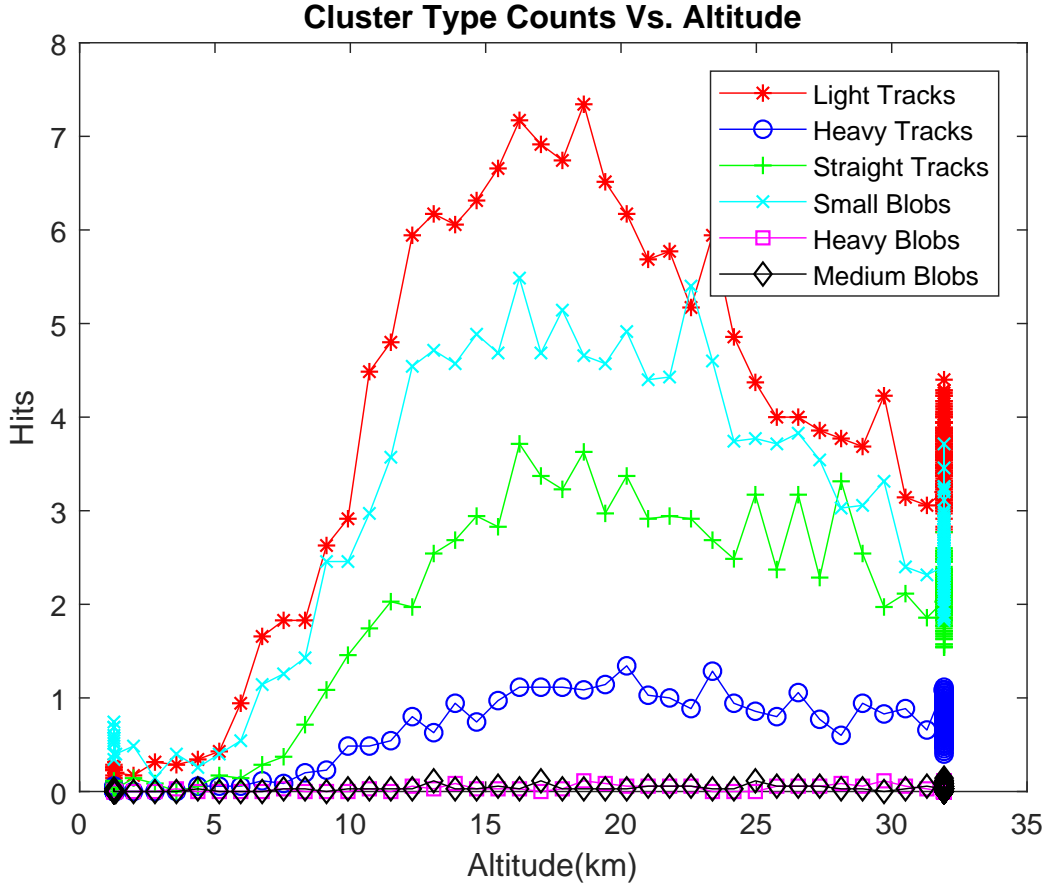


Figure 7: Distribution of cluster type counts versus altitude for the duration of the 2018 flight.

The distribution of cluster types as they vary with altitude is shown in Figure 7.







Type	Inner Pixels	Length/ Width Ratio	Other Criteria	Example Tracks
Small Blob	0	-	1 or 2 Pixels, 3 if L shape, 4 is square	
Heavy Track	> 4	> 1.25	Not S.Blob Density > 0.3	
Heavy Blob	> 4	< 1.25	Not H.Track Density > 0.5	
Medium Blob	> 1	< 1.25	Not H.Blob Density > 0.5	
Straight Track	0	> 8	Not M.Blob Minor axis < 3 pixels	
Light Track	-	-	Not S.Track	

Figure 8: Cluster types CITE ME FROM STUART

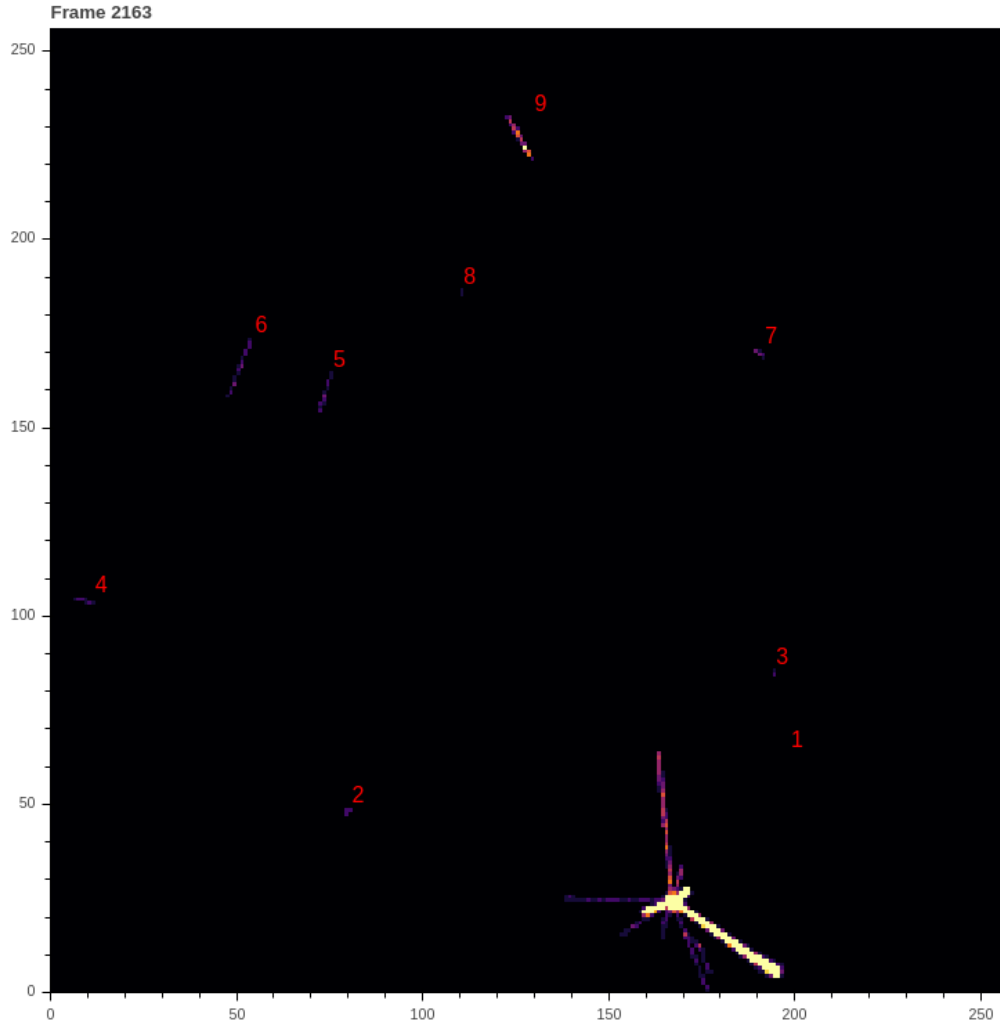


Figure 9: Single MiniPIX frame collected at float on the 2017 flight.

Figure 9 shows one of many particle tracks recorded during the 2017 flight, while both flights recorded many frames similar to this. The track lengths of ionizing particles can be calculated and used to directly measure the linear energy transfer of various primary and secondary particles.

## 4. Discussion

One of the primary goals of the SORA flights was to successfully utilize the MiniPIX device in dosimetric applications. The figures presented in Section 3 clearly demonstrate this success as the results from the two missions are validated by comparison to previous stratospheric balloon flights. The BEXUS [5] balloon flights have shown that Medipix sensors are able to perform in the stratosphere. NASA’s RaD-X missions [21] provided results to which SORA’s data can be compared.

### *4.1. System Performance*

Due to the lack of heat convection in the stratosphere, a pressing concern regarding the functionality of the MiniPIX was the temperature of the device at float altitude. The device is guaranteed to operate within the manufacturer’s limits of 0 °C to 70 °C. With the use of a relatively compact heatsink, the temperature of the device remained within 10 °C to 40 °C. The success of the heatsink suggests that less material could be utilized, consequently reducing the overall size of the apparatus.

### *4.2. Space Weather*

The radiation environment in the Earth-Moon system has become a cause for concern over the last several years as comparisons between the levels of solar radiation during the solar cycle have been made. The increase in length of the solar minimum phase, and subsequent decrease in duration of the solar maximum, corresponds to record high cosmic ray activity. A comparison between the number of days a 30 year old male could spend in interplanetary

space in the 1990's versus 2014 revealed a substantial decrease from 1000 days in the 1990's to approximately 700 in 2014. [10].

The collected data associated with radiation exposure to commercial flight attendants and pilots provides another reason to monitor cosmic ray activity. The United States National Council on Radiation Protection Measurements reported, between 2003-2006, flight crews as having the highest average effective dose among terrestrial radiation workers. And a 2015 epidemiology study revealed a 70 % increase in the risk of miscarriages in flight attendants who received 0.1 mGy or more in their first trimester. While there is a wealth of compelling data that strongly suggests a need to monitor radiation exposure, flight crews remain the only occupational group exposed to unqualified and undocumented levels over the duration of their careers. [12].

While there are physics-based aviation radiation models, there are several major issues with even the most current models. Depending on the dosimetric quantities used, the variation in agreement between the measured and model data ranges from within 10% to over 50%. Accurately representing primary cosmic ray particles incident at the top of the atmosphere, and subsequent secondary particle production interactions and transport processes at all altitudes above commercial flight levels, and the lack of measurements covering a range of atmospheric altitudes, latitudes, and solar cycle activity, are all necessary to render exposure predictions similar to those measured at aviation altitudes [11].

Space radiation and GCRs pose real health risks to astronauts and pilots in any field. With the increase in cosmic ray flux in the Earth Moon system, radiation exposure in LEO and the atmosphere must be monitored to ensure



they do not exceed the occupational dose limits. The ability to measure real-time exposure is arguably a crucial tool that can help mitigate increased health risks. Additionally, Studying radiation types and dose levels near the nebulous border between space and Earth’s atmosphere, and within the various zones of the atmosphere, facilitates preparation for current and future space missions; and aviation in general.

#### *4.3. Success of SORA to Similar Experiments*

The success of the application of the MiniPIX as a dosimeter is clearly seen with direct comparison to the RaD-X missions. The RaD-X flights were characteristically very similar to the SORA flights in that both missions were launched from Fort Sumner, New Mexico, had similar float altitudes, and had similar flight durations. RaD-X utilized a RaySure monitor to measure the dose during the balloon flight. The MiniPIX is able to acquire data from the same variety of particles species as RaySure with the exception of neutron interactions. However, the MiniPIX is able to be modified with a scintillating material in order to indirectly detect neutrons, as shown in [19] and [20]. Unlike the RaySure, the MiniPIX is able to record the track length of incident particles. The LET spectrum can be calculated using the deposited particle energy measured by the detector as well as the track length of the energy deposition. Quality factors regarding the dose equivalent can be extracted from the LET spectrum. Thus, the dose equivalent can be calculated only using data measured by the MiniPIX whereas conventional methods require the use of Monte Carlo simulations [16] or additional equipment.

Figure 5b aligns beautifully with Figure 3 presented by RaD-X [21]. Both figures show the absorbed dose as a function of altitude and the Regener-

Pfotzer Maximum is visible in all data sets. The absorbed dose measured by SORA is slightly higher than that measured by RaD-X. This can be explained by the difference of the year of each flight and the relationship between the solar cycle and GCR flux. The solar cycle is inversely related to GCR flux [22], i.e. if the sun is at solar minimum then the GCR flux is at a maximum. The RaD-X mission was in 2015 during the decline of the current solar cycle, solar cycle 24. Solar cycle 24 hit its solar minimum in March 2018, only a few months prior to the second SORA flight in September 2018.

The results of the SORA missions touched upon various points highlighted at the conclusion of RaD-X. The scientists behind the RaD-X missions stressed the importance of a cheap and compact dosimeter, as the importance of dosimetric measurements are being realized beyond scientific applications. The quasi-commercial availability of the MiniPIX makes the device a strong candidate for such applications.

There is much to be learned beyond the applications of SORA. For example, the radiation shielding provided by Earth's atmosphere at SORA's float altitude is similar to that provided by the Martian atmosphere at the surface of Mars [21]. By better understanding the complex nature of the radiation field in the stratosphere, humanity can better prepare for our exploration on Mars. Further applications also include dose measurements for aviation as the need for such use was outlined by our discussion of space weather.

## **5. Conclusion**

Both 2017 and 2018 high altitude balloon flights proved successful. The MiniPIX gathered a wealth of data after flying for 19.5 h at altitudes between

30 km and 40 km. In the 2017 flight, dose rate peaked at approximately  $4.8 \mu\text{Gy h}^{-1}$  while the 2018 flight dose rate peaked at  $4.8 \mu\text{Gy h}^{-1}$ . Flying at altitudes beyond 30 km, both flights observed the Pfozter-Regener maximum. Overall, the MiniPIX device performed beyond expectations, proving to function adequately in the upper atmosphere, but also successfully operating as a low-cost device for dosimetry applications.

## 6. Acknowledgements

Dr. T. Gregory Guzik @ LSU Louisiana Space Group for supporting HASP flights

NASA Balloon Program Office for supporting HASP flights

NASA Columbia Scientific Balloon Facility for supporting HASP flights

University of Houston Physics Department

University of Houston Biology and Microbiology Department

University of Houston STEM Center

Dr. Jacobs at the UH STEM Center

Randy Clark at the UH Science Center Machine Shop - Lab Machinist

## 7. Funding Sources

This work was supported by the University of Houston STEM Center.

- [1] Regener E. & Pfozter G., *Vertical Intensity of Cosmic Rays by Threefold Coincidences in the Stratosphere.*, Nature 136, 718-719, (1935).
- [2] W. Friedberg, K. Copeland, What Aircrews Should Know About Their Occupational Exposure to Ionizing Radiation, available

- at [https://www.faa.gov/data\\_research/research/med\\_humanfacs/oamtechreports/2000s/media/0316.pdf](https://www.faa.gov/data_research/research/med_humanfacs/oamtechreports/2000s/media/0316.pdf) (accessed on February 1st, 2019).
- [3] B. Grajewski, E. A. Whelan, C. C. Lawson, M. J. Hein, et al., Miscarriage Among Flight Attendants, *Epidemiology*, 26 (2015) 192–203.
  - [4] N. A. Schwadron, J. B. Blake, A. W. Case, C. J. Joyce, et al., Does the worsening galactic cosmic radiation environment observed by CRAFT preclude future manned deep space exploration? *Space Weather*, 12, (2014) 622 - 632.
  - [5] J. Urbar, J. Scheirich, J. Jakubek, Medipix/Timepix cosmic ray tracking on BEXUS stratospheric balloonflights. *Nucl. Instrum. Methods A*, 633 (2011) 206 - 209.
  - [6] N. Stoffle, L. Pinsky, M. Kroupa, S. Hoang, et al., Timepix-based radiation environment monitor measurements aboard the International Space Station. *Nucl. Instrum. Methods Phys. Res., A*, 782 (2015) 143 - 148.
  - [7] source for image: Measurement of the energy resolution and calibration of hybrid pixel detectors with GaAs:Cr sensor and Timepix readout chip - Scientific Figure on ResearchGate. Available from: [https://www.researchgate.net/figure/a-Structure-of-a-Timepix-detector-b-Timepix-pixel-detector-with-USB-interface/fig3\\_270906129](https://www.researchgate.net/figure/a-Structure-of-a-Timepix-detector-b-Timepix-pixel-detector-with-USB-interface/fig3_270906129) [accessed 23 Apr, 2019]
  - [8] High Altitude Student Platform, available at <http://laspace.lsu.edu/hasp/> (accessed on April 21, 2019).

- [9] ADVACAM, available at <http://www.advacam.com> (accessed on February 2nd, 2017).
- [10] The Worsening Cosmic Ray Situation, available at <https://spaceweatherarchive.com/2018/03/05/the-worsening-cosmic-ray-situation/> (accessed on March 6th, 2019).
- [11] C. J. Mertens, Overview of the Radiation Dosimetry Experiment (RaD-X) flight mission, *Space Weather*, 14 (2018) 921 – 924.
- [12] N. A. Schwadron, F. Rahmanifard, J. WilsonB., A. P. Jordan et al., Update on the Worsening Particle Radiation Environment Observed by CRaTER and Implications for Future Human Deep-Space Exploration, *Space Weather*, 16 (2018) 289 – 303.
- [13] B. J. Lewis, M. J. McCall, A. R. Green, L. G. I. Bennett, M. Pierre, U. J. Schrewe, K. O’Brien, E. Felsberger, Aircrew Exposure from Cosmic Radiation on Commercial Airline Routes, *Radiation Protection Dosimetry*, 93 (2001) 293 – 314.
- [14] C. Granja, S. Pospisil, Quantum dosimetry and online visualization of X-ray and charged particle radiation in commercial aircraft at operational flight altitudes with the pixel detector Timepix, *Advances in Space Research*, 54 (2014) 241 - 251.
- [15] Medipix collaboration, available at <https://medipix.web.cern.ch/> (accessed on April 21, 2019).

- [16] S. George, Dosimetric Applications of Hybrid Pixel Detectors, available at <https://ro.uow.edu.au/cgi/viewcontent.cgi?article=5605&context=theses> (accessed on April 21, 2019).
- [17] ADVACAM, MINIPIX Version 1.0 Datasheet, available at <http://advacam.com/system/wp-content/uploads/2017/05/MiniPIX-Datasheet-v2-45fps-2017-11-08.pdf> (accessed on April 21, 2019).
- [18] J. Jakubek, Precise energy calibration of pixel detector working in time-over-threshold mode, Nucl. Instrum. Methods Phys. Res., A, 633 (2011) 262 - 266.
- [19] P. Masek, J. Jakubek, J. Uher, R. Prestond, Directional detection of fast neutrons by the Timepix pixel detector coupled to plastic scintillator with silicon photomultiplier array, Journal of Instrumentation, 8 (2013).
- [20] J. Uher, Ch. Fröjdh, T. Holý, J. Jakubek, S. Petersson, S. Pospíšif, G. Thungström, D. Vavřík, and Z. Vykydal, Silicon Detectors for Neutron Imaging, AIP Conference Proceedings, 958 (2007) 101 - 104.
- [21] A. D. P. Hands, K. A. Ryden, C. J. Mertens, The disappearance of the pfotzer-regener maximum in dose equivalent measurements in the stratosphere, Space Weather, 14 (2016) 776 - 785.
- [22] D. H. Hathaway, The Solar Cycle, Living Reviews in Solar Physics, 12 (2015).